文章编号：1001-9014(XXXX)XX-0001-08

DOI:10.11972/j.issn.1001-9014.XXXX.XX.001

Efficient multi-millijoule THz wave generation from laser interactions with a cylindrical GaAs waveguide

Zahra Ghanavati, Hamid Reza Zangeneh[1*]

(Department of Photonics and Plasmas, Faculty of Physics, University of Kashan, Kashan 8731753153, Iran)

Abstract: This study involved a comprehensive investigation aimed at achieving efficient multi-millijoule THz wave generation by exploiting the unique properties of cylindrical GaAs waveguides as effective mediators of the conversion of laser energy into THz waves. Through meticulous investigation, valuable insights into optimizing THz generation processes for practical applications were unearthed. By investigating Hertz potentials, an eigenvalue equation for the solutions of the guided modes (i.e., eigenvalues) was found. The effects of various parameters, including the effective mode index and the laser pulse power, on the electric field components of THz radiation, including the fundamental TE (transverse electric) and TM (transverse magnetic) modes, were evaluated. By analyzing these factors, this research elucidated the nuanced mechanisms governing THz wave generation within cylindrical GaAs waveguides, paving the way for refined methodologies and enhanced efficiency. The significance of cylindrical GaAs waveguides extends beyond their roles as mere facilitators of THz generation; their design and fabrication hold the key to unlocking the potential for compact and portable THz systems. This transformative capability not only amplifies the efficiency of THz generation but also broadens the horizons of practical applications.

Key words: terahertz waves, cylindrical waveguides, gallium arsenide (GaAs) matter, nonlinear optical processes, multi-millijoule THz pulses

Introduction

In recent years, the quest for high-power and efficient generation of terahertz (THz) wave radiation has garnered significant attention due to its diverse applications spanning from spectroscopy and imaging to telecommunications and beyond. The unique properties of THz radiation, such as its non-ionizing nature and ability to penetrate various materials, make it an indispensable tool in numerous fields [1-4]. Among the myriad techniques explored for THz wave generation, nonlinear optical processes triggered by ultrafast laser-matter interactions emerge as standout contenders, offering promising avenues for realizing efficient and controllable THz sources. In this issue, semiconductor materials such as gallium arsenide (GaAs) have garnered significant attention due to their advantageous nonlinear optical properties and seamless integration with established laser technologies [5-7]. Leveraging these properties, GaAs-based waveguides have risen to prominence as an exceptionally compelling strategy for unlocking efficient THz generation capabilities. The allure of semiconductor materials such as GaAs lies in their inherent nonlinear response to intense laser fields, enabling the exploitation of various nonlinear optical phenomena that are crucial for THz wave generation [8-10]. GaAs, with its strong nonlinear susceptibility and high damage threshold, provides an ideal platform for the efficient conversion of optical energy into THz radiation. Furthermore, its compatibility with well-established laser systems ensures seamless integration into existing experimental setups, facilitating the exploration of novel THz generation schemes. Within this framework, by confining a laser beam within a waveguide structure, the interaction length between the laser pulse and the nonlinear medium is effectively extended, enhancing the efficiency of THz wave generation. Additionally, the waveguide geometry enables precise control over the generated THz radiation's spatial distribution and temporal characteristics, facilitating tailored applications across a broad spectrum of disciplines.

To develop low-cost packaging technology for coherent power combining in the THz regime, Sumer Makhlouf et al. proposed a novel 3D multilayer design integrating an array of InP-based THz photodiodes with a

Received date: 2025-01-02, **revised date**: 2025-03-17 收稿日期:2025-01-02,修回日期:2025-03-17

Biography: Zahra Ghanavati (1989-), female, Iran, PhD student. Her research focuses on the simulation of nonlinear photonic processes, particularly for efficient THz wave generation using advanced waveguide structures. E-mail: zahra.ghanavati90@gmail.com

[*] **Corresponding author**: Hamid Reza Zangeneh is an Associate Professor in the Photonics and Plasmas Department, which he established at the University of Kashan. His research interests include nonlinear optics, integrated photonics, optical measurements, and imaging. E-mail: hrzangeneh@kashanu.ac.ir

rectangular waveguide power combiner [11]. K. Gallacher and colleagues found that double metal waveguides had lower losses for Ge/SiGe THz quantum cascade laser gain media, requiring gain thresholds of 15.1 cm^{-1} and 23.8 cm^{-1} to produce a 4.79 THz laser at 10 K and 300 K, respectively [12]. V. Georgiadis et al. designed dielectric-lined rectangular waveguides for THz phase velocity matching with electron bunches, and they confirmed them experimentally through time-frequency analysis [13]. A. V. Mitrofanov's team studied the polarization and spatial mode structure of THz radiation driven by mid-infrared wavelengths, showing that a two-color laser driver alters the spatial polarization mode structure based on the gas pressure [14]. Joselito E. Muldera's research demonstrated robust THz emission from titanium-doped lithium niobate waveguides, suggesting that these could replace conventional THz emitters [15]. Giacomo Balistreri's study on broadband THz pulses via a tapered two-wire waveguide indicated that the input THz pulse was reshaped into its first-order time integral waveform, and the operational spectral range was tunable by adjusting the output gap size and tapering angle [16]. Varun Pathania et al. developed a waveguide for a small-scale free-electron laser with a small eye-shaped cross-section, enhancing the FEL gain by increasing the interaction between the electron beam and radiation [17]. Basem Y. Shahriar's team presented waveguided spintronic THz emitters that demonstrated up to 87% modulation of generated THz power by varying the optical pump polarization angle [18]. Linzheng Wang and colleagues used simulations to generate gigawatt-level THz emission by injecting a weakly relativistic ultrashort laser into a parabolic plasma channel, identifying two fundamental mechanisms: linear-mode conversion from laser wakefields and electromagnetic waveguide mode excitation, resulting in linearly and radially polarized THz emissions [19].

Among the numerous techniques for THz generation, nonlinear optical procedures induced by ultrafast laser-matter interactions stand out as promising avenues. The generation of THz waves through laser-driven mechanisms involves the exploitation of nonlinear optical effects such as optical rectification and difference frequency generation. The interaction of intense laser pulses with GaAs waveguides presents a compelling mechanism for THz wave generation. This context builds upon previous studies in the field of THz wave generation and extends the investigation to the realm of cylindrical GaAs waveguides. When an intense femtosecond laser pulse interacts with a suitable nonlinear medium, such as GaAs, nonlinear polarization is induced, leading to the emission of THz radiation through various nonlinear processes. GaAs, with its favorable nonlinear optical properties and high damage threshold, emerges as a prominent candidate for efficient THz wave generation. This study addresses the efficient generation of multi-millijoule THz waves through laser interactions with cylindrical GaAs waveguides. Understanding the interplay among laser parameters, the cylindrical geometry of the waveguide, and THz output characteristics are crucial for tailoring the generation process to specific applications. The utilization of cylindrical waveguides offers distinct advantages over planar geometries, including enhanced light confinement and improved interaction lengths, leading to heightened nonlinear optical conversion efficiencies. Moreover, the cylindrical geometry of the waveguide allows for precise control over the spatial and temporal properties of the generated THz radiation, enabling tailored applications in spectroscopy, imaging, and beyond. By exploiting the unique properties of cylindrical GaAs waveguides, we demonstrate a significant enhancement in THz output energies. This article is organized as follows: In Section 1, the theory of the mechanism of THz radiation in GaAs waveguides is considered. A discussion of the results, consisting of THz fields and the properties of THz emissions, is presented in Section 2. Conclusions are drawn in Section 3.

1 Mechanism of THz Radiation in GaAs waveguides

A laser pulse, polarized linearly, is precisely concentrated at the entrance of a cylindrical waveguide aligned with the z-axis. Within a GaAs waveguide that is encased in air, electrons undergo acceleration, ultimately transforming their energy into a relativistic half-cycle THz radiation pulse. Typically, multiple optical modes are stimulated concurrently, with their strengths being primarily contingent upon the waveguide's radius. In our setup using a micro-scale waveguide, the majority of laser energy is directed into the fundamental waveguide mode. In the context of Hertz potentials, Π^e and Π^μ represent the electric and magnetic potentials, respectively. They play a crucial role in comprehending the interaction and propagation of electromagnetic waves within materials. The electric field $\vec{E}$ can be derived from the electric Hertz potential Π^e as:

$$\vec{E} = -\vec{\nabla}\left(\vec{\nabla} \cdot \overrightarrow{\Pi^e}\right) - \frac{\partial^2 \Pi^e}{\partial t^2} \quad . \quad (1)$$

Similarly, the magnetic field $\vec{H}$ can be derived from the magnetic Hertz potential Π^μ as:

$$\vec{H} = -\vec{\nabla}\left(\vec{\nabla} \cdot \overrightarrow{\Pi^\mu}\right) - \frac{\partial^2 \Pi^\mu}{\partial t^2} \quad . \quad (2)$$

Consequently, the electromagnetic fields can be formulated in terms of these two Hertz potentials as follows:

$$E_z = \frac{\partial^2 \Pi^e}{\partial z^2} + k^2 \Pi^e \,, H_z = \frac{\partial^2 \Pi^\mu}{\partial z^2} + k^2 \Pi^\mu \quad , \quad (3a)$$

$$E_\rho = \frac{\partial^2 \Pi^e}{\partial z \partial \rho} - i\omega\mu \frac{1}{\rho} \frac{\partial \Pi^\mu}{\partial \varphi} \,, H_\rho = \frac{\partial^2 \Pi^\mu}{\partial z \partial \rho} + i\omega\mu \frac{1}{\rho} \frac{\partial \Pi^e}{\partial \varphi} \,, \quad (3b)$$

$$E_\varphi = \frac{1}{\rho} \frac{\partial^2 \Pi^e}{\partial z \partial \varphi} + i\omega\mu \frac{\partial \Pi^\mu}{\partial \rho} \,, H_\varphi = \frac{1}{\rho} \frac{\partial^2 \Pi^\mu}{\partial z \partial \varphi} - i\omega\mu \frac{\partial \Pi^e}{\partial \rho} \,. \quad (3c)$$

In the two regions, the general solutions for the Hertz potentials are obtained as follows:

$$\Pi^{e\mu}_{GaAs}(\rho,\varphi,z) = \sum\nolimits_n \mathrm{A}^{e\mu}_n J_n\left(\frac{\kappa_G \rho}{a}\right) \Phi^{e\mu}_n(\varphi) e^{-i\gamma z}, \quad (4a)$$

$$\Pi^{e\mu}_{Air}(\rho,\varphi,z) = \sum\nolimits_n \mathrm{B}^{e\mu}_n H_n\left(\frac{\kappa_A \rho}{a}\right) \Phi^{e\mu}_n(\varphi) e^{-i\gamma z}, \quad (4b)$$

where $\Phi^e_n(\varphi) = \sin\varphi$, $\Phi^\mu_n(\varphi) = \cos\varphi$, $\kappa_G = \sqrt{k_G^2 - \gamma^2}\, a$,

$\kappa_A = \sqrt{k_A^2 - \gamma^2}\, a$, k_G and k_A are the wave numbers of GaAs and air media, and J_n and H_n are the Bessel functions. At the boundary $r = a$ between the two regions, the tangential components of both $\vec{E}$ and $\vec{H}$ would remain continuous. This requirement leads to four linear homogeneous simultaneous equations for the coefficients, which are formulated as follows:

$$\kappa_G^2 J_n(\kappa_G) A_n^e - \kappa_A^2 H_n(\kappa_A) B_n^e = 0 \quad , \quad (5a)$$

$$\kappa_G^2 J_n(\kappa_G) A_n^\mu - \kappa_A^2 H_n(\kappa_A) B_n^\mu = 0 \quad , \quad (5b)$$

$$n\gamma J_n(\kappa_G) A_n^e + i\omega\mu\kappa_G J_n'(\kappa_G) A_n^\mu - n\gamma H_n(\kappa_A) B_n^e - i\omega\mu\kappa_A H_n'(\kappa_A) B_n^\mu = 0 \quad , \quad (5c)$$

$$n\gamma J_n(\kappa_G) A_n^\mu + i\omega\varepsilon_G\kappa_G J_n'(\kappa_G) A_n^e - n\gamma H_n(\kappa_A) B_n^\mu - i\omega\varepsilon_A\kappa_A H_n'(\kappa_A) B_n^\mu = 0 \quad . \quad (5d)$$

To obtain nonzero solutions for $A_n^{e,\mu}$ and $B_n^{e,\mu}$, the determinant of the coefficients should be equal to zero; as a result, the following eigenvalue equation can be cast as:

$$\left(\frac{J_n'(\kappa_G)}{\kappa_G J_n(\kappa_G)} - \frac{H_n'(\kappa_A)}{\kappa_A J_n(\kappa_A)}\right)\left(\frac{J_n'(\kappa_G)}{\kappa_G J_n(\kappa_G)} - \frac{\varepsilon_A H_n'(\kappa_A)}{\varepsilon_G\kappa_A J_n(\kappa_A)}\right) - n^2\left(\frac{1}{\kappa_G^2} - \frac{1}{\kappa_A^2}\right)\left(\frac{1}{\kappa_G^2} - \frac{\varepsilon_A}{\varepsilon_G\kappa_A^2}\right) = 0 \quad . \quad (6)$$

This equation precisely delineates the frequency dependence. To solve this equation with respect to κ_G, it is advantageous to establish the following relationship between κ_G and κ_A:

$$\kappa_A = -i\sqrt{n_f^2 - \kappa_G^2} \quad , \quad (7)$$

where $n_f = \sqrt{\kappa_G^2 - \kappa_A^2}\, a = n_a\kappa_G a$ is the normalized frequency parameter or n_f number, and n_a is the numerical aperture, which is defined as follows:

$$n_a = \sqrt{1 - \frac{\varepsilon_A}{\varepsilon_G}} \quad . \quad (8)$$

Thus, one recognizes that for the GaAs waveguide in this scheme, the permittivity is constant and n_a remains constant, while n_f varies proportionally with the frequency. Additionally, for a guided mode, the electromagnetic field in the radial direction must decay exponentially, indicating that the solutions for κ_A should be purely imaginary. This results in the restriction condition of $\kappa_G < n_f$. To find the solutions of the guided modes, i. e., eigenvalues, Eq. (4) is rewritten as follows:

$$[J(n) + K(n)][F(n) - 2G(n)] + n_a^2 K(n) G(n) = 0 \quad , (9)$$

where the recursion formula of the Bessel function, $J_n'(x) = nJ_n(x)/x - J_{n+1}(x)$, is used, and other functions are defined as follows:

$$F(n) = J(n) + K(n) + n_a^2\left[\frac{n}{y^2} - K(n)\right], \quad (10a)$$

$$G(n) = \frac{n}{\kappa_G^2} + \frac{n}{y^2} \quad , \quad (10b)$$

$$J(n) = \frac{J_{n+1}(\kappa_G)}{\kappa_G J_n(\kappa_G)} \quad , \quad (10c)$$

$$K(n) = \frac{K_{n+1}(y)}{yK_n(y)} \quad , \quad (10d)$$

where $K(y)$ is the modified Hankel function, and $y = \sqrt{n_f^2 - \kappa_G^2}$. For the GaAs waveguide, since n_f is proportional to ω, κ_G also varies considerably with ω in the THz region, which describes how quickly the electromagnetic wave attenuates as it propagates through the waveguide. This variation is essential to understand when designing and analyzing optical devices based on GaAs waveguides. In the high-frequency desired region, n_a approaches zero, and the equation becomes:

$$\frac{J_{n+1}(\kappa_G)}{\kappa_G J_n(\kappa_G)} + \frac{K_{n+1}(y)}{yK_n(y)} = 0 \quad , \quad (11a)$$

$$\frac{J_{n-1}(\kappa_G)}{\kappa_G J_{n-2}(\kappa_G)} + \frac{K_{n-1}(\kappa_G)}{\kappa_G K_{n-2}(\kappa_G)} = 0 \quad . \quad (11b)$$

The equations above provide two sets of the eigenvalue x corresponding to two guided modes with the same mode number n. One is the "high-n mode", and the other is the "low-n mode". We utilized MATLAB software and COMSOL Multiphysics for comprehensive modeling and analysis.

2 Results and discussion

The THz portion of the electromagnetic radiation spectrum has become a focal point in scientific exploration due to its unique properties and potential applications. One approach for generating THz radiation involves exploiting nonlinear interactions within materials under the influence of intense laser fields. This method has attracted significant interest among researchers, driven by the rising demand for compact, tabletop-scale THz sources. To meet this demand, scientists are exploring innovative approaches to design such sources. Among these, the utilization of cylindrical GaAs waveguides has emerged as a promising solution. These waveguides offer an efficient means of converting laser energy into THz waves, thereby enhancing the overall efficiency of the generation process. Moreover, their design facilitates practical scalability, paving the way for widespread adoption. The advent of cylindrical GaAs waveguides not only improves efficiency but also enables the development of compact and portable THz generation systems. This innovation holds particular significance for applications requiring on-site or mobile THz imaging and spectroscopy, such as security screening, industrial inspection, and field research. By leveraging cylindrical GaAs waveguides, researchers can create versatile THz systems capable of delivering high-quality imaging and spectroscopic data in diverse environments. In light of these advancements, the present study delves into the effective generation of multi-millijoule THz waves through laser interactions with cylindrical GaAs waveguides. By investigating this phenomenon, researchers aim to further optimize THz generation processes, unlocking new possibilities for practical applications in various fields. To implement simulation runs, the following experimental parameters were considered: a short laser pulse (> 50 fs) at a wavelength of λ = 800 nm with an energy parameter of 4.3 J. The laser focal length was 1.5 m with a focal spot size of r_L = 22 μm at FWHM, which provided a peak in-

tensity of $I_0 = 6.2 \times 10^{15}$ W/cm^2. While THz generation using GaAs is not entirely new, the specific use of cylindrical GaAs waveguides as a medium for efficient THz generation is a novel aspect. The claim of generating multi-millijoule THz waves is significant and suggests a substantial improvement over previous methods or configurations. The use of cylindrical waveguides is proposed to improve light confinement and increase interaction length, leading to higher nonlinear optical conversion efficiencies. The cylindrical geometry is claimed to offer better control over the spatial and temporal properties of the generated THz radiation, potentially enabling new applications. Essentially, the novelty lies in the specific configuration (cylindrical GaAs waveguide) and the resulting enhancement in THz generation efficiency and controllability.

In this study, the geometric parameters of the cylindrical GaAs waveguide, including its radius and length, were carefully selected to optimize THz wave generation. These parameters were chosen based on a combination of theoretical predictions and prior experimental results. The selected dimensions ensure optimal light confinement and interaction length while balancing fabrication feasibility and material properties. Comparative analysis with planar and alternative cylindrical designs highlighted the advantages of the chosen parameters. To determine the optimal geometric parameters, we employed its robustness in handling multi-dimensional optimization problems. The algorithm was designed to maximize the THz output while adhering to practical constraints. The objective function incorporated factors such as light confinement efficiency and THz conversion efficiency. We implemented this algorithm, allowing us to systematically explore the parameter space and identify the optimal configuration. The results were validated by confirming the effectiveness of the optimized design.

A schematic illustration of the interaction of the laser beam with the GaAs waveguide is depicted in Fig. 1, which shows the laser beam being directed into or through the GaAs waveguide, depicting how the light propagates, reflects, or interacts within the waveguide structure. This interaction could be crucial for various applications such as optical communication, laser technology, or photonic integrated circuits. In Fig. 2, the 3D emission of THz waves is depicted for different effective mode indices to demonstrate how changes in confinement and dispersion alter the way the waves propagate within the GaAs waveguide. As the figure shows, the changes in the way the waves propagate occur because the effective mode index affects the confinement and dispersion of the waves within the waveguide. The effective mode index in a waveguide is a measure of how fast light travels through the waveguide compared with its speed in a vacuum. It is essentially a way to characterize the propagation properties of light within the waveguide structure. A higher effective mode index typically indicates stronger confinement, meaning that the waves are more tightly bound to the waveguide construction. As the effective mode index changes, the confinement of the waves within the waveguide also changes, leading to variations in how the waves spread and propagate. In addition, the effective mode index also affects the dispersion characteristics of the waveguide. Dispersion refers to how the speed of light varies with its frequency as it travels through the waveguide. Different effective mode indices correspond to different dispersion properties, which can cause the waves to spread out or concentrate differently as they propagate through the waveguide. By visualizing these changes, researchers can gain insights into how to optimize waveguide designs for specific applications, such as THz communication or sensing.

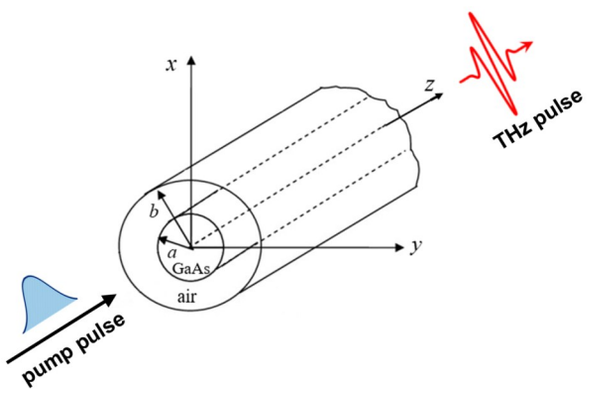

Fig. 1 Schematic illustration of the interaction of the laser beam with the GaAs waveguide

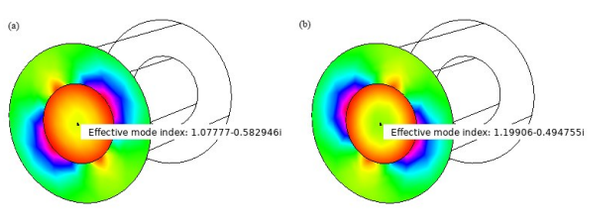

Fig. 2 The 3D emission of THz waves in the GaAs waveguide for different effective mode indices

The x- and y-components of the THz electric field in the 2D cross-section of the GaAs waveguide for $n = 1$ and the in-plane mode are shown in Figs. 3 and 4 for various wavelengths. Similarly, the z-component for the out-of-plane mode is depicted in Fig. 5. The in-plane and out-of-plane modes represent different field orientations relative to the waveguide structure, providing insights into THz wave propagation. As the wavelength increases, the energy transfer rate also increases, suggesting changes in waveguide dispersion. Dispersion, which describes how the light speed varies with wavelength in a medium, affects wave guidance and confinement. Longer wavelengths may experience less dispersion, improving the waveguiding efficiency. Additionally, the increasing number of peaks and better wave confinement at higher wavelengths highlight the interplay of dispersion, material properties, and waveguide design in shaping THz wave propagation within the GaAs waveguide.

Figure 6 illustrates the variations in the κ_G parame-

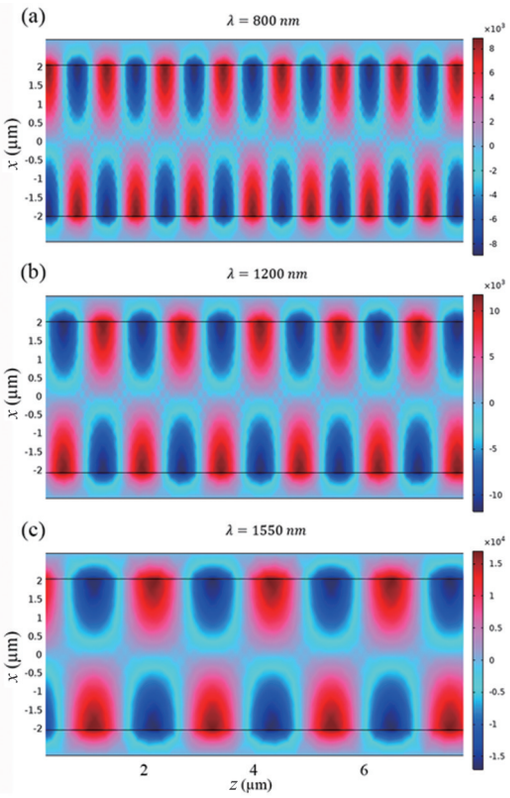

Fig. 3 The variations in the x-component of the electric field of THz radiation in the 2D cross-section of the GaAs waveguide for n = 1 in the in-plane mode with various wavelengths

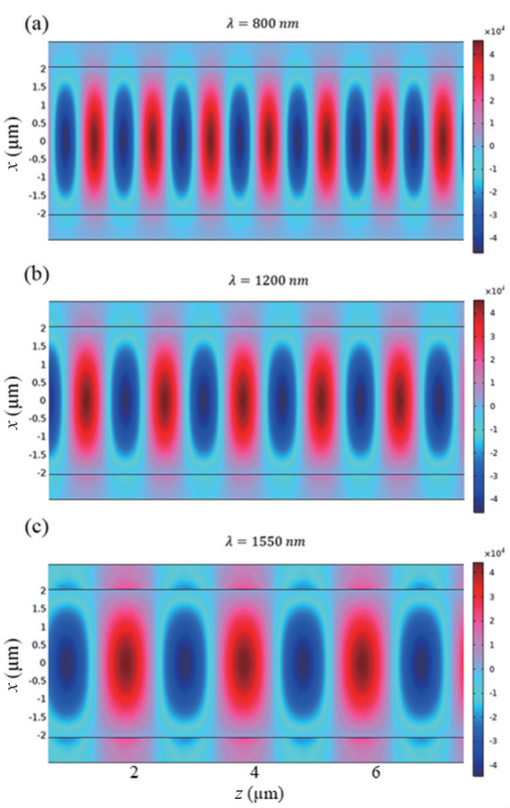

Fig. 4 The variations in the y-component of the electric field of THz radiation in the 2D cross-section of the GaAs waveguide for n = 1 in the in-plane mode with various wavelengths

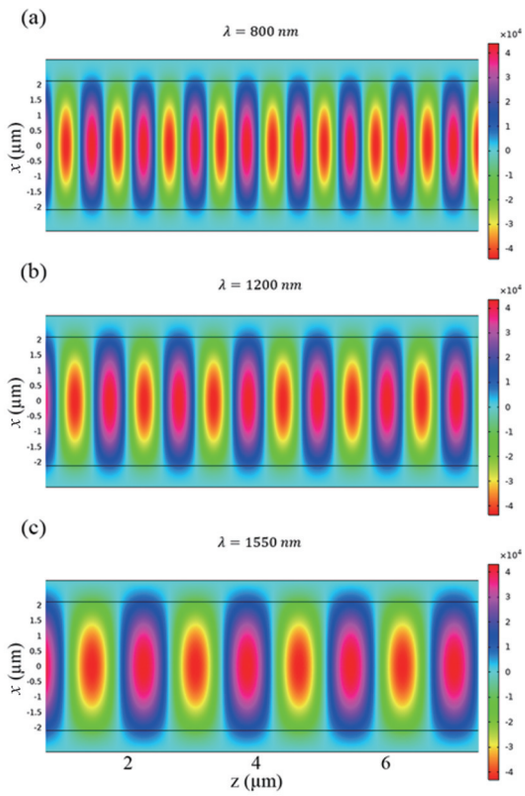

Fig. 5 The variations in the z-component of the electric field of THz radiation in the 2D cross-section of GaAs waveguide for n = 1 in the out-of-plane mode with various wavelengths

ter versus the normalized frequency for different n-modes, calculated using MATLAB. The figure reveals that as n-modes increase, the propagation constant rises, intermediate oscillations decrease, and the diffusion reaches saturation more quickly. Higher n-modes correspond to faster wave propagation, smoother variations in κ_G, and earlier stabilization of propagation characteristics due to reduced oscillations. Diffusion saturation, where the propagation constant stabilizes with frequency, occurs at lower frequencies for higher n-modes, enhancing waveguide performance. The coupling coefficient (κ_G) reflects energy transfer between modes, with phase mismatch and material dispersion in GaAs at low frequencies leading to a negative coupling coefficient due to the inefficient energy coupling and destructive interference.

Figures 7 and 8 show the x- and y-components of the THz electric field in the 2D cross-section of a GaAs waveguide for various in-plane modes, while Fig. 9 depicts the z-component for out-of-plane modes. Increasing n-modes enhances oscillations and THz wave propagation due to higher-order modes with more complex spatial distributions and higher propagation constants. Higher-order modes exhibit more electric field oscillations and propagate faster within the waveguide, as shown in Figs. 7-9. These effects are critical for optimizing GaAs waveguides in THz applications like communication, sensing, and imaging.

Figure 10 illustrates the normalized power spectral amplitudes of THz emission measured in the far field as a

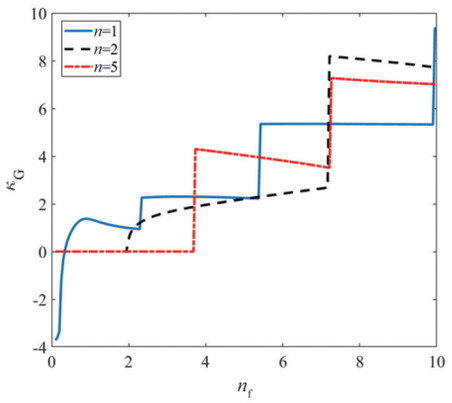

Fig. 6 The variations in the κ_G parameter versus the normalized frequency parameter for different n-modes

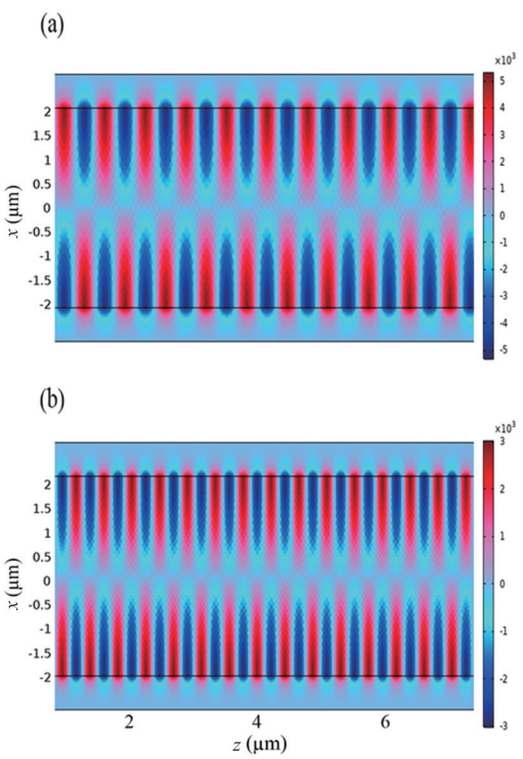

Fig. 7 The variations in the x-component of the electric field of THz radiation in the 2D cross-section of the GaAs waveguide for various in-plane modes

function of frequency for three different excitation laser wavelengths: 800 nm, 1 200 nm, and 1 550 nm. The x-axis represents the THz frequency (THz), while the y-axis indicates the normalized amplitude (a. u.), which reflects the relative intensity of the emitted THz waves. The spectral profiles reveal a clear correlation between the efficiency of THz generation and the laser wavelength. The 800 nm laser produces the highest peak amplitude, centered around 3. 5 THz, with a relatively narrow spectral bandwidth. The 1 200 nm laser results in an intermediate peak intensity at approximately 3 THz, accompanied by a broader spectral distribution. The 1 550 nm laser exhibits the lowest peak intensity but covers the broadest spectral range, extending toward lower

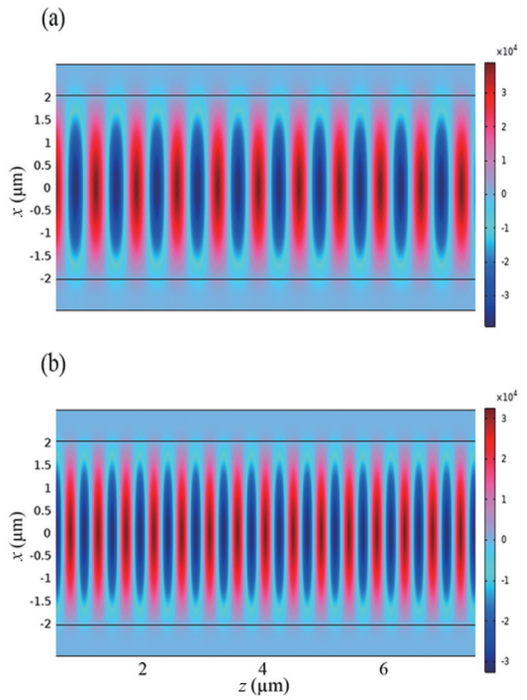

Fig. 8 The variations in the y-component of the electric field of THz radiation in the 2D cross-section of the GaAs waveguide for various in-plane modes

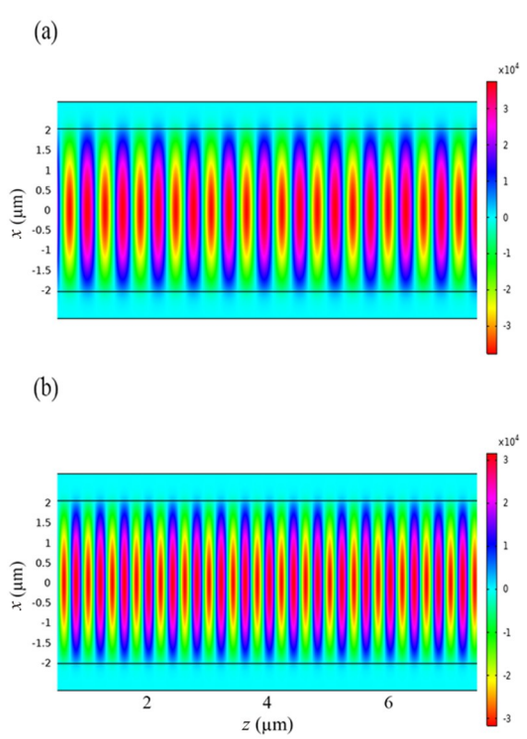

Fig. 9 The variations in the z-component of the electric field of THz radiation in the 2D cross-section of the GaAs waveguide for various out-of-plane modes

frequencies. The shaded region highlights the spectral range of interest (0. 1-5 THz), where efficient THz generation is observed. These findings confirm that shorter excitation wavelengths lead to higher THz intensities with

narrower bandwidths, whereas longer wavelengths contribute to spectral broadening at the cost of reduced peak intensity. The far-field measurements provide essential insights into optimizing laser parameters for efficient THz wave generation in GaAs-based waveguides.

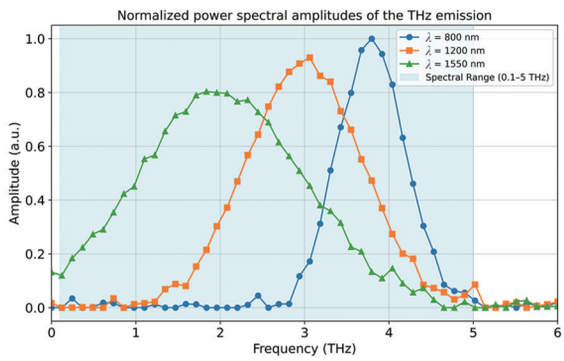

Fig. 10 Normalized spectral amplitudes of THz emission recorded in the far field

Table 1 summarizes the crystals used for nonlinear frequency conversion, detailing the waveguiding geometry employed to confine the THz radiation, the spectral range of the generated frequencies, and the corresponding conversion efficiency. As mentioned, our approach utilizes GaAs as the waveguide material with a cylindrical geometry, achieving a broad spectral range of 0. 1-5 THz. This wide spectral range enhances the versatility of the generated THz waves for various applications requiring a wide bandwidth in the THz domain. Also, our study delivers a competitive conversion efficiency of 6.65×10^{-5} W^{-1}, which is a well-balanced conversion efficiency compared to other studies.

In general, to achieve the high THz conversion efficiency, the waveguide and laser parameters must be carefully optimized. The analysis suggests that the excitation wavelength of 800 nm is the most effective, as it provides the strongest nonlinear response and the highest peak THz intensity. Efficient THz generation also depends on the selection of fundamental and first higher-order modes, which facilitate the energy transfer while minimizing dispersion losses. The use of short laser pulses, in the range of 50 fs to 100 fs, is beneficial in broadening the spectral range and enhancing the THz radiation. Moreover, the simulations indicate that an optimal phase-matching condition, represented by the κ_G value of approximately 7.5, maximizes coupling efficiency and mode interactions, leading to higher THz power output. Additionally, the peak laser intensity of 6.2×10^{15} W/cm^2, achieved through the tight focal spot size of 22 μm (FWHM) and the focal length of 1.5 m, ensures strong nonlinear polarization and energy conversion. This configuration enables strong THz wave generation with enhanced spectral bandwidth and improved conversion efficiency.

3 Conclusions

This investigation of efficient multi-millijoule THz wave generation through laser interactions with cylindrical GaAs waveguides marks a substantial leap forward in advancing the capabilities of THz technology. This study accurately examines the intricate mechanisms underlying THz wave generation and underscores the pivotal role played by cylindrical GaAs waveguides in amplifying THz generation efficiency. The proposed system possesses a spectral range of 0. 1-5 THz, proving its versatility in various THz applications needing wide bandwidth, and describes a competitive conversion efficiency of 6.65×10^{-5} W^{-1} beyond many existing configurations. By harnessing the unique properties of GaAs waveguides, researchers are empowered to develop compact, portable THz systems tailored to meet the demands of diverse applications. This study highlights the versatility and scalability of GaAs waveguides, offering practical solutions for tabletop-scale THz sources that cater to the burgeoning need for adaptable THz technologies. Through a thorough exploration of several parameters, such as wavelength, effective mode index, and number of modes, this research clarifies the nuanced dynamics governing THz wave propagation within GaAs waveguides. These insights not only inform the optimization of THz generation processes but also pave the way for the realization of high-fidelity imaging and spectroscopic capabilities across a spectrum of fields, including security screening, industrial inspection, and field research. Furthermore, this study emphasizes the pivotal role of higher-order modes in augmenting the oscillation rate and propagation efficiency of THz waves within GaAs waveguides. By elucidating the significance of these modes, this research offers invaluable visions for enhancing the performance of GaAs waveguides for a wide array of THz applications. Through continued investigation and refinement, researchers stand poised to unlock the full potential of

Table 1 Compare several waveguiding configurations for THz wave generation

Study/Reference	Waveguide Material	Waveguide Geometry	Spectral range of generation	Conversion efficiency
Mei et al. [20]	GaAs	ridge	1.59 – 2.66 THz	5.62×10^{-5} W^{-1}
Yang et al. [21]	LiNbO3	embedded arrangement	2.7 – 3.6 THz	3.5×10^{-4} W^{-1}
Vodopyanov et al. [22]	GaAs	planar dielectric	2.07 THz	5.3×10^{-6} W^{-1}
Marandi et al. [23]	GaAs	embedded arrangement	≤ 3.5 THz	4.2×10^{-5} W^{-1}
Chen et al. [24]	graphene/AlGaAs	buried-channelrib	5 – 7 THz	0.5×10^{-6} W^{-1}
Zhu et al. [25]	poled polymer	cylindrical	< 0.95 THz	–
This work	GaAs	cylindrical	0.1 – 5 THz	6.65×10^{-5} W^{-1}

GaAs waveguides, ushering in a new era of innovation and advancement in THz technology.

References

[1] ZHU J-F, DU C-H, HUANG T-J, et al. Free-electron-driven beam-scanning terahertz radiation [J]. Optics Express, 2019, 27(18): 26192-26202.

[2] WANG W, LU P-K, VINOD A K, et al. Coherent terahertz radiation with 2.8-octave tunability through chip-scale photomixed microresonator optical parametric oscillation [J]. Nature Communications, 2022, 13(1): 5123.

[3] GE H, SUN Z, JIANG Y, et al. Recent advances in THz detection of water [J]. International Journal of Molecular Sciences, 2023, 24(13): 10936-10958.

[4] JIN J, XIONG H, ZHOU J, et al. Strong-field THz radiation-induced curing of composite resin materials in dentistry [J]. Biomedical Optics Express, 2023, 14(5): 2311-2323.

[5] GHALGAOUI A, REIMANN K, WOERNER M, et al. Resonant second-order nonlinear terahertz response of gallium arsenide [J]. Physical Review Letters, 2018, 121(26): 266602.1-266602.6.

[6] CHANG L, BOES A, PINTUS P, et al. Low loss (Al) GaAs on an insulator waveguide platform [J]. Optics Letters, 2019, 44(16): 4075-4078.

[7] SURESH M I, SCHWEFEL H G, VOGT D W. Gallium arsenide whispering gallery mode resonators for terahertz photonics [J]. Optics Express, 2023, 31(20): 33056-33063.

[8] SANTOS R D, OZAWA S, MAG-USARA V, et al. Cherenkov-phase-matched nonlinear optical detection and generation of terahertz radiation via GaAs with metal-coating [J]. Optics Express, 2016, 24(22): 24980-24988.

[9] NANDI U, DUTZI K, DENINGER A, et al. ErAs: In (Al) GaAs photoconductor-based time domain system with 4.5 THz single shot bandwidth and emitted terahertz power of 164 μW [J]. Optics letters, 2020, 45(10): 2812-2815.

[10] HALE L L, JUNG H, GENNARO S D, et al. Terahertz pulse generation from GaAs metasurfaces [J]. ACS photonics, 2022, 9(4): 1136-1142.

[11] MAKHLOUF S, STEEG M, HADDAD T, et al. Novel 3-D multilayer terahertz packaging technology for integrating photodiodes arrays and rectangular waveguide-power combiners [J]. IEEE Transactions on Microwave Theory and Techniques, 2020, 68(11): 4611-4619.

[12] GALLACHER K, ORTOLANI M, REW K, et al. Design and simulation of losses in Ge/SiGe terahertz quantum cascade laser waveguides [J]. Optics Express, 2020, 28(4): 4786-4800.

[13] GEORGIADIS V, HEALY A, HIBBERD M, et al. Dispersion in dielectric-lined waveguides designed for terahertz-driven deflection of electron beams [J]. Applied Physics Letters, 2021, 118(14): 144102.1-144102.5.

[14] MITROFANOV A, VORONIN A, ROZHKO M, et al. Polarization and spatial mode structure of mid-infrared-driven terahertz-to-microwave radiation [J]. ACS Photonics, 2021, 8(7): 1988-1996.

[15] MULDERA J E, AFALLA J P C, FURUYA T, et al. Creating terahertz pulses from titanium-doped lithium niobate-based strip waveguides with 1.55 μm light [J]. Journal of Materials Science: Materials in Electronics, 2021, 32(18): 23164-23173.

[16] BALISTRERI G, TOMASINO A, DONG J, et al. Time-domain integration of broadband terahertz pulses in a tapered two-wire waveguide [J]. Laser & Photonics Reviews, 2021, 15(8): 2100051.1-2100051.10.

[17] PATHANIA V, BAE S, JANG K-H, et al. Low-loss and small-cross-section waveguide for compact terahertz free-electron laser [J]. Optics Continuum, 2022, 1(1): 91-102.

[18] SHAHRIAR B Y, HOPMANN E, ELEZZABI A Y. On-Chip Waveguided Spintronic Sources of Terahertz Radiation [J]. ACS Photonics, 2023, 10(2): 518-525.

[19] WANG L, CHEN Y, ZHANG G, et al. Tunable High-Field Terahertz Radiation from Plasma Channels [J]. Laser & Photonics Reviews, 2023, 17(6): 2200627.

[20] MEI J, ZHONG K, XU J, et al. Efficient terahertz generation via GaAs hybrid ridge waveguides [J]. IEEE Photonics Technology Letters, 2019, 31(20): 1666-1669.

[21] YANG J, WANG C. Efficient terahertz generation scheme in a thin-film lithium niobate-silicon hybrid platform [J]. Optics Express, 2021, 29(11): 16477-16486.

[22] VODOPYANOV K, AVETISYAN Y H. Optical terahertz wave generation in a planar GaAs waveguide [J]. Optics letters, 2008, 33(20): 2314-2316.

[23] MARANDI A, DARCIE T E, SO P P. Design of a continuous-wave tunable terahertz source using waveguide-phase-matched GaAs [J]. Optics express, 2008, 16(14): 10427-10433.

[24] CHEN T, WANG L, CHEN L, et al. Tunable terahertz wave difference frequency generation in a graphene/AlGaAs surface plasmon waveguide [J]. Photonics Research, 2018, 6(3): 186-192.

[25] ZHU W, AGRAWAL A, CAO H, et al. Generation of broadband radially polarized terahertz radiation directly on a cylindrical metal wire [J]. Optics Express, 2008, 16(12): 8433-8439.